

Article



http://pubs.acs.org/journal/acsodf

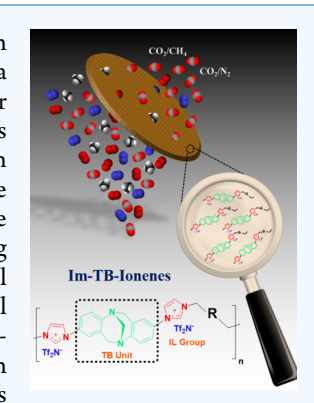
# Design and Synthesis of Imidazolium-Mediated Tröger's Base-Containing Ionene Polymers for Advanced CO<sub>2</sub> Separation **Membranes**

Irshad Kammakakam, † Kathryn E. O'Harra, † Jason E. Bara, \*, † and Enrique M. Jackson †

<sup>†</sup>Department of Chemical & Biological Engineering, University of Alabama, Tuscaloosa, Alabama 35487-0203, United States \*NASA Marshall Space Flight Center, Huntsville, Alabama 35812, United States

Supporting Information

ABSTRACT: It is highly desirable to integrate the CO<sub>2</sub> solubility benefits of ionic liquids (ILs) in polymeric membrane systems for effective CO<sub>2</sub> separations. Herein, we are exclusively exploring a series of four novel imidazolium-mediated Tröger's base (TB)-containing ionene polymers for enhanced CO<sub>2</sub> separation. The two diimidazole-functionalized Tröger's base monomers synthesized from "ortho"- and "para"-substituted imidazole anilines were polymerized with equimolar amounts of two different aromatic and aliphatic comonomers ( $\alpha,\alpha'$ -dichloro-p-xylene and 1,10-dibromodecane, respectively) via Menshutkin reactions to obtain four respective ionene polymers ([Im-TB(o&p)-Xy][Cl] and ([Im-TB(o&p)-C<sub>10</sub>][Br], respectively). The resulting ionene polymers having halide anions were exchanged with [Tf2N] anions, yielding a novel Tröger's base material [Im-TB(x)-R][Tf<sub>2</sub>N] or "Im-TB-Ionenes". The structural and physical properties as well as the gas separation behaviors of the copolymers of aromatic and aliphatic Im-TB-Ionenes have been extensively investigated with respect to the regiochemistry of imidazolium groups at the ortho and para positions of the TB unit. The imidazolium-mediated TB-Ionenes showed high CO<sub>2</sub> solubility and hence an excellent CO<sub>2</sub>/CH<sub>4</sub> permselectivity of 82.5. The Im-TB-Ionenes also displayed good thermal and mechanical stabilities.



## 1. INTRODUCTION

Membrane-based gas separation utilizing polymeric materials has undoubtedly been at the forefront of separation processes such as hydrogen recovery in ammonia manufacture (H<sub>2</sub>/N<sub>2</sub> and  $H_2/CH_4$ ),  $CO_2$  capture and sequestration  $(CO_2/H_2, CO_2/H_3)$  $N_2$ , and  $CO_2/CH_4$ ),  $N_2$  or  $O_2$  enrichment of air  $(O_2/N_2)$ , and olefin/paraffin separations in petrochemical industries (C<sub>3</sub>H<sub>6</sub>/ C<sub>3</sub>H<sub>8</sub>). 1-6 In general, polymeric membrane-based gas separation is flexible, easy to scale up, and energy-efficient. However, for a given gas pair, a strong inherent trade-off between permeability (the product of the diffusivity and solubility coefficients) and selectivity (the product of the diffusivity and solubility selectivities) invariably affects the polymer membranes and limits the gas separation performance.7-9 Improving separation performance of polymeric membranes in aggressive feeds such as natural gas upgrading (i.e., CO<sub>2</sub>/ light gas separations) is of great interest and an enduring challenge in gas separation processes. To prepare highly CO<sub>2</sub>permeable membranes, polymers with a high diffusivity coefficient and/or a high solubility coefficient must be designed.

Polymers consisting of high-free-volume elements often yield high diffusion coefficients and enhance the permeability. A class of soluble microporous polymers having rigid ladderlike chains containing sites of contortion, so-called polymers of intrinsic microporosity (PIMs), is well known for their high fractional free volume (FFV) and high gas permeabilities. 10

Recent developments in the design of microporous polymers have turned to the use of Tröger's base (TB) derivatives as versatile new building blocks for the synthesis of extraordinary gas separation membranes. 15–20 Several approaches such as TB polymerization 15-17 and TB-based copolymers 18-20 have been proposed to incorporate TB units into the polymer backbone. In general, the TB moiety is a nitrogen-containing kinked heterocycle with a V-shaped bridged bicyclic linking group, a chiral molecule with a site of contortion that can rigidify the polymer chain and generate microporosity in polymer matrixes. Results revealed that TB-containing polymer backbones can obtain much higher CO<sub>2</sub> permeabilities due to the large disruptions in chain packing (i.e., increased FFV) caused by V-shaped tertiary (3°) amine diazocine bridges and improve the overall gas transport properties, particularly for CO<sub>2</sub>/CH<sub>4</sub> separation with the performance surpassing the Robeson upper bound curves. 17-20

On the other hand, polymeric membranes either containing or built from ionic liquids (ILs) have recently emerged as promising CO<sub>2</sub> separation materials due to their high CO<sub>2</sub> solubility and high CO2 gas selectivities over N2 and CH4. Several promising approaches have been applied toward combining ILs with polymer membranes, including supported

Received: December 31, 2018 Accepted: February 4, 2019 Published: February 15, 2019



ionic liquid membranes (SILMs), 21-23 polymerized IL monomers,<sup>24</sup> IL copolymers,<sup>25</sup> pendant-IL functionalization,<sup>26</sup> and IL composite membranes.<sup>27</sup> Initial interest in the use of ILs essentially focused on the examination of SILMs, in which ILs are impregnated into microporous polymers to achieve high CO<sub>2</sub> permeability as well as high CO<sub>2</sub>/N<sub>2</sub> selectivity.<sup>22</sup> The use of SILMs in practical gas separation processes, however, is hindered by stability issues as ILs can easily leach out from the membranes at pressure differences below 1 atm. <sup>28</sup> Meanwhile, membranes prepared from polymeric ILs, also known as poly(IL)s, have become of greater interest than SILMs for CO<sub>2</sub> separation because of their moderate gas separation properties and superior mechanical properties. Poly(IL)s are not specifically ILs but rather are polymers containing several forms of ionic salts with many features shared with ILs, such as their high CO<sub>2</sub> solubility. Poly(IL)s also offer a high CO2 sorption capacity and high sorption and desorption rates compared to ILs. 29,30

We have recently focused on the design and synthesis of various imidazole-functionalized monomers that are integrated into a different type of poly(IL), called ionenes, an IL-inspired platform where the polymer backbone contains cationic groups. In our previous work, we have successfully demonstrated the introduction of imidazolium cations into the rigid polyimide (PI) backbone via Menshutkin reactions to form PI—ionene hybrids or "ionic polyimides".<sup>31</sup> Membranes prepared from these newly developed ionic polyimides displayed high CO<sub>2</sub> separation properties, together with excellent mechanical and thermal stabilities.

In the present work, we combine the benefits of the abovementioned TB-based polymers and ILs to produce a novel imidazolium-mediated Tröger's base-containing ionene polymer for enhanced  $CO_2$  separation. To the best of our knowledge, this is the first example of using sterically hindered TB-based-imidazole monomers (Im-TB(o) and Im-TB(p), Figure 1) to synthesize ionene polymers for selective  $CO_2$ 

(4,10-Diimidazo methano dibenzo-diazocine) (2,8-Diimidazo methano dibenzo-diazocine)

**Figure 1.** Tröger's base-containing diimidazole monomers used in this study.

separation. The newly designed ionenes yielded high-molecular-weight polymers and displayed excellent thermal and mechanical properties, together with enhanced separation performance for  $\mathrm{CO_2/CH_4}$  and  $\mathrm{CO_2/N_2}$  gas pairs. We also investigated the effects of two different aliphatic and aromatic comonomers ( $\alpha$ , $\alpha'$ -dichloro-p-xylene and 1,10-dibromode-cane, respectively) used in these TB-Ionene polymers, which impacted the physical properties as well as the gas separation behaviors of the corresponding polymer membranes.

#### 2. RESULTS AND DISCUSSION

**2.1. Synthesis of Tröger's Base-Containing Imidazole Monomers (Im-TBs, III).** The Tröger's base monomers (III) having "ortho"- and "para"-substituted diimidazole were synthesized via a three-step synthetic route, starting from

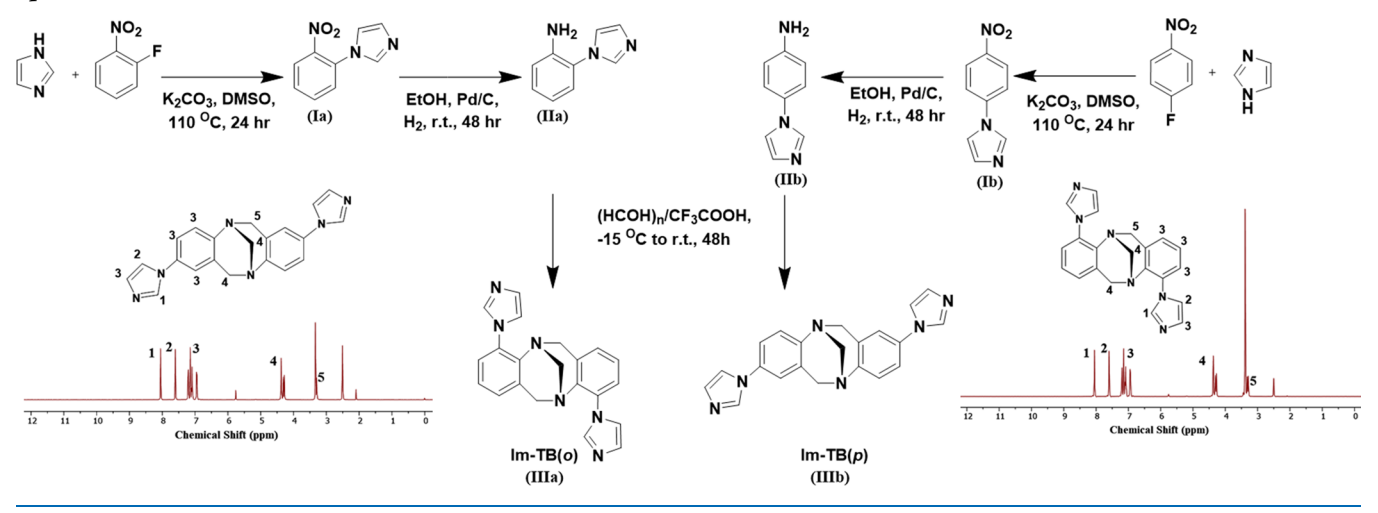
commercially available imidazole and either 2-fluoronitrobenzene (2-FNB) or 4-fluoronitrobenzene (4-FNB) to afford IIIa and IIIb, respectively (Figure 1). The intermediates (imidazole-aniline derivatives, IIa and IIb) were first synthesized through the reaction between imidazole and 2-FNB or 4-FNB in the presence of K<sub>2</sub>CO<sub>3</sub> in DMSO at 110 °C, followed by the Pd/C-catalyzed H2 reduction in EtOH at ambient temperature. The purity and molecular structures of compounds IIa and IIb were confirmed by <sup>1</sup>H NMR (Figures S1 and S2, Supporting Information). The desired Im-TBs were further synthesized by the condensation reaction between II and paraformaldehyde in the presence of trifluoroacetic acid (TFA) under ambient conditions. As previously reported, a mixture of enantiomers  $(R_iR$  and  $S_iS)$  can be possible for Im-TBs (III) due to the presence of a V-shaped 3° amine diazocine bridge.<sup>32</sup> Direct comparisons of IIIa and IIIb with their enantiomers, however, were not considered in this study as Im-TBs exclusively prepared for polymerization. Nevertheless, both IIIa and IIIb were purified via recrystallization with DCM-MeOH mixtures. The purity and structures of Im-TBs were confirmed by H<sup>1</sup> NMR (Scheme 1).

2.2. Synthesis and Characterization of Imidazolium-Mediated TB-Based Ionene Polymers (Im-TB-Ionene). As summarized in Scheme 2, a series of four novel imidazoliummediated Tröger's base-containing ionene polymers (Im-TB-Ionenes) were synthesized. The two diimidazole-functionalized Tröger's base monomers synthesized from ortho- and parasubstituted imidazole anilines were first polymerized with equimolar amounts of two different aromatic and aliphatic comonomers ( $\alpha,\alpha'$ -dichloro-p-xylene and 1,10-dibromodecane, respectively) via Menshutkin reactions to obtain four corresponding ionene polymers ([Im-TB(o&p)-Xy][Cl] and ([Im-TB(o&p)-C<sub>10</sub>][Br], respectively). The resulting ionene polymers having halide anions were further exchanged with [Tf<sub>2</sub>N] anions, yielding novel Tröger's base-containing ionene materials Im-TB-Ionenes. All the Im-TB-Ionene polymers were found to have very high number average molecular weights (e.g., m/z = 169843.8 for [Im-TB(p)-C<sub>10</sub>][Tf<sub>2</sub>N]), as confirmed by high-resolution MALDI-TOF, Figures S3-S6), and similarly, high number average molecular weights were also reported in our previous works.<sup>31,33</sup> The qualitative and quantitative characterizations of newly developed Im-TB-Ionene polymers were further analyzed by <sup>1</sup>H NMR, FTIR, and thermogravimetric analysis (TGA)

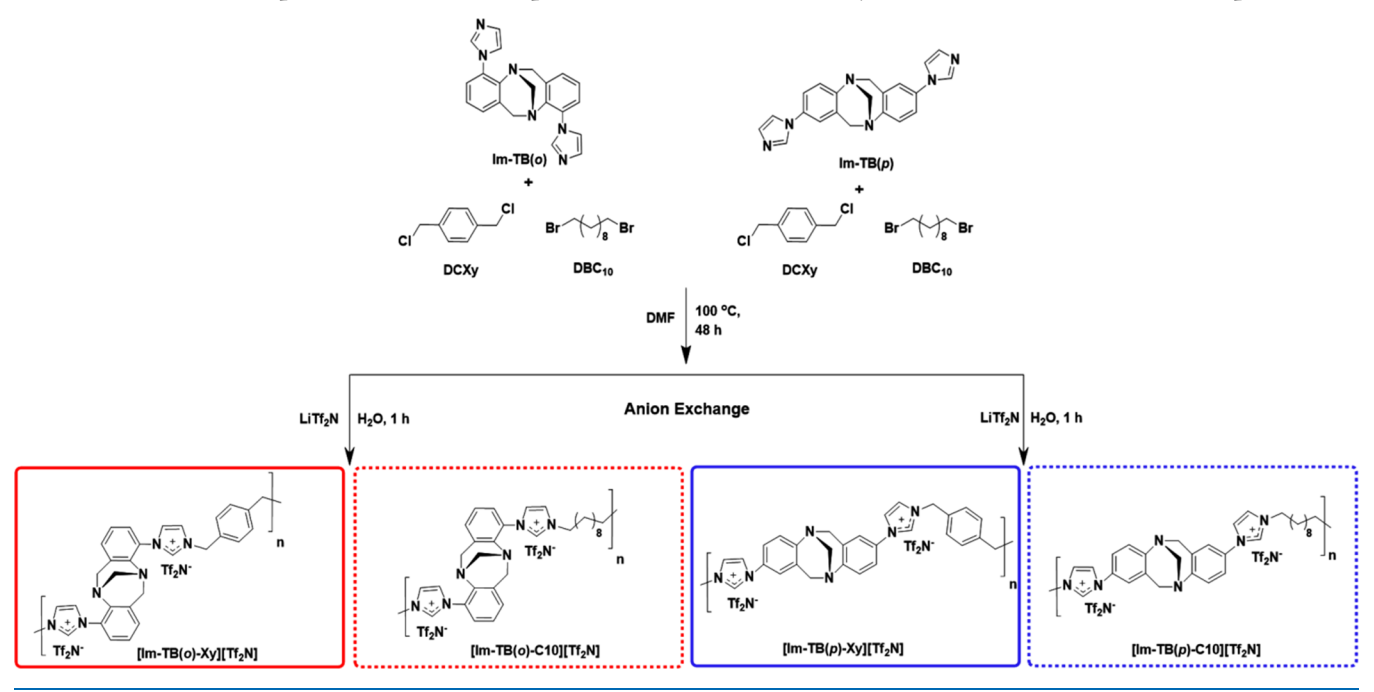
The <sup>1</sup>H NMR spectra of all four Im-TB-Ionene polymers were consistent with their proposed chemical structures. As shown in Figure 2, the <sup>1</sup>H NMR spectra of the Im-TB-Ionene polymers display characteristic peaks of imidazolium protons  $(H_a)$  at 10.0 ppm and the bicyclic ring of Tröger's base protons  $(H_b)$  in the region of 3.5–5.5 ppm, indicating the successful incorporation of imidazolium–TB groups in the polymer backbone. At the same time, benzylic protons  $(H_c$  at 5.5 ppm) of  $[\text{Im-TB}(o\&p)\text{-Xy}][\text{Tf}_2\text{N}]$  and alkyl chain protons  $(H_c$  at 1.2 ppm) of  $[\text{Im-TB}(o\&p)\text{-C}_{10}][\text{Tf}_2\text{N}]$  were confirmed due to the presence of aromatic and aliphatic groups in the respective polymer backbones, proving the structures of newly developed Im-TB-Ionene polymers (Figure 2).

As shown in Figure 3, the chemical structures of Im-TB-Ionene polymers were further verified by FT-IR. All four Im-TB-Ionene polymers showed the corresponding peaks of aromatic TB groups (C-H, C-N, and C=C stretching vibrations at 3082, 1690, and 1480 cm<sup>-1</sup>, respectively) as well

Scheme 1. Schematic Representation of the Preparation of Tröger's Base-Containing Diimidazole Monomers and Their NMR Spectra



Scheme 2. Schematic Representation of the Preparation of Im-TB-Ionene Polymers with Their Various Counterparts



as ionic moieties such as imidazolium cations (C–N vibrations at  $1320~{\rm cm}^{-1})$  and  $[Tf_2N]^-$  anions (SO $_2$  and SNS stretching vibrations at 1190 and 1050 cm $^{-1}$ , respectively), indicating that the imidazolium-based TB-Ionene polymers having  $[Tf_2N]^-$  counteranions were successfully formed. On the other hand, the new peaks corresponding to the aliphatic groups (C–H stretching vibrations at 2860 cm $^{-1}$ ) were only found for  $[{\rm Im} TB({\it o\&p}) - C_{10}][Tf_2N]$  polymers, confirming the structural variations in newly developed Im-TB-Ionene polymers.

The thermal stabilities of Im-TB-Ionene polymers were evaluated by thermogravimetric analysis (TGA) under a  $\rm N_2$  atmosphere (Figure 4). All six Im-TB-Ionene polymers exhibited very similar thermograms with two-stage degradations, the first of which occurring between 350 and 480 °C was attributed to the decomposition of the major ionene backbone, followed by the evolution of the residual ionic char at approximately 480–650 °C. In general, the TGA results

showed that Im-TB-Ionene polymers are highly stable and adequate for gas separation applications.

**2.3. Membrane Fabrication of Im-TB-Ionene Polymers.** The Im-TB-Ionene polymers displayed high solubility in common polar aprotic solvents including DMAc, DMSO, and NMP (Table S1, Supporting Information). The excellent solubility indicated the compatibility of the newly developed ionene materials to form thin films. The corresponding membranes were prepared by casting a DMAc solution of respective Im-TB-Ionene polymers, followed by vacuum drying to give dense, transparent, and flexible membranes (the optical images are shown in Figure 5). Before use for characterization tests, the membranes were washed with hexane and dried for 24 h under ambient conditions to remove any residual solvents. The thickness of the Im-TB-Ionene membranes was controlled to be 90 to 110  $\mu$ m.

**2.4. Physical Properties of Im-TB-Ionene Polymers.** The effect on thermal transitions of Im-TB-Ionene polymers as

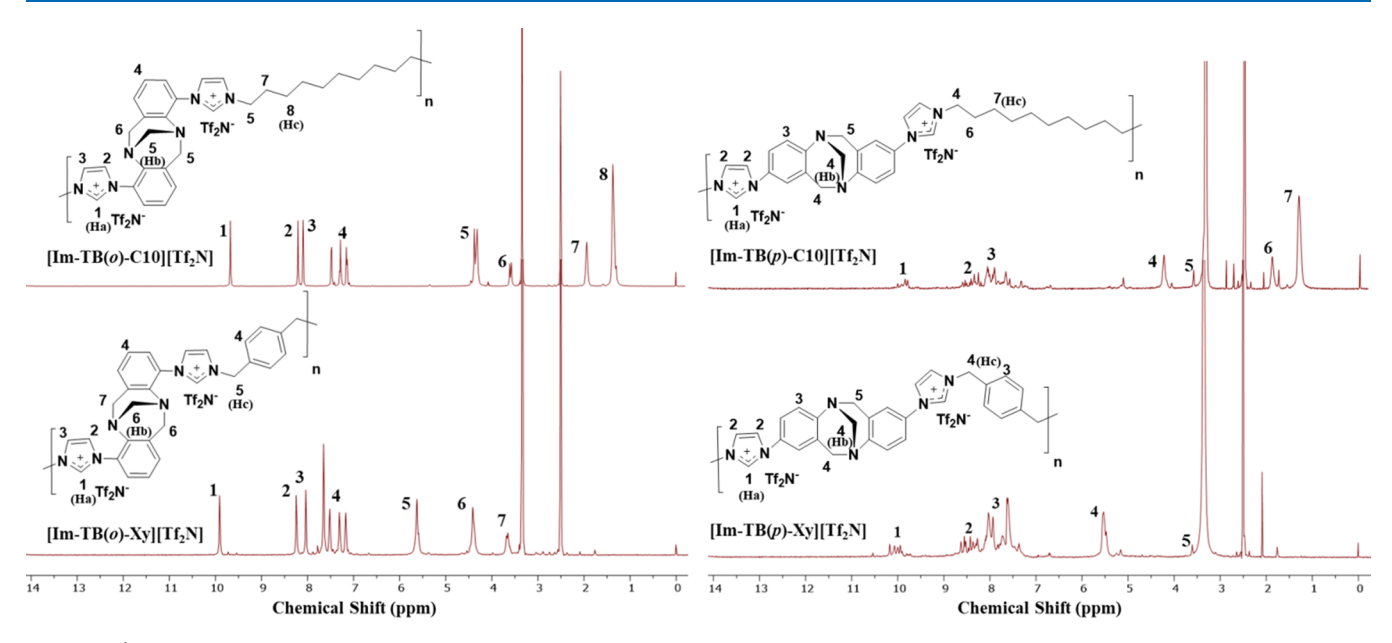


Figure 2. <sup>1</sup>H NMR spectra of the Im-TB-Ionene polymers.

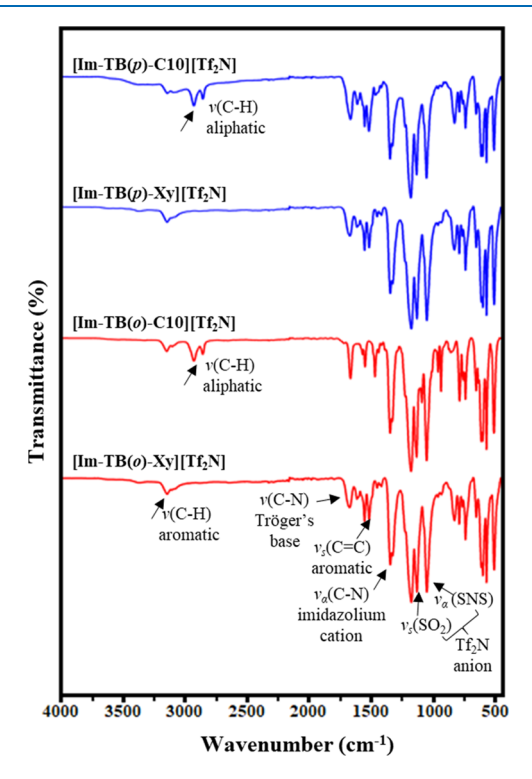


Figure 3. FT-IR spectra of the Im-TB-Ionene polymers.

a function of imidazolium groups as well as hard and soft segments (aromatic and aliphatic comonomers, respectively) was investigated using DSC analysis (Table 1 and Figure 6). The ionic polymers often yield lower glass transition temperature ( $T_g$ ) values, which is proportional to the ratio of the counterion charge to the distance between the centers of cations and anions. Interestingly, in the newly developed Im-TB-Ionenes, the aromatic hard segments containing ionenes ([Im-TB(o&p)-Xy][Tf<sub>2</sub>N]) possessed a similar high  $T_g$  around 100 °C, which was even much higher than those obtained from other imidazolium—ionenes. Although slightly lower  $T_g$  values ( $\leq 80$  °C) were observed for the aliphatic soft segment [Im-

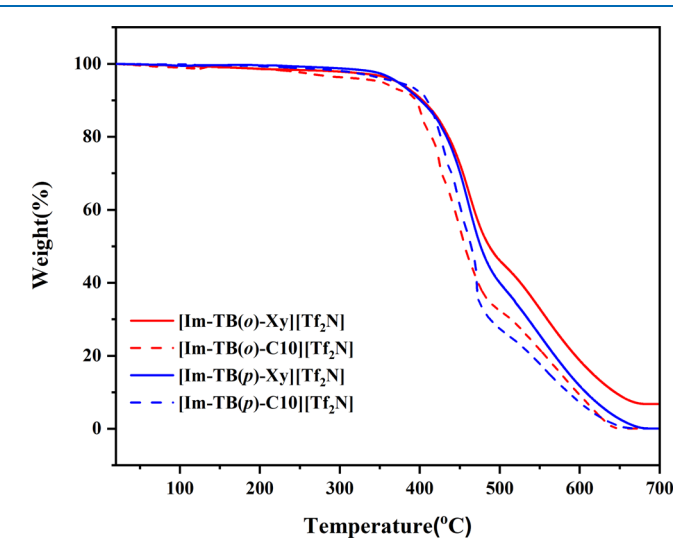


Figure 4. TGA curves of the Im-TB-Ionene polymers.



**Figure 5.** Photographs of Im-TB-Ionene polymer membranes (diameter = 47 mm).

Table 1. Physical Parameters Characterizing the Im-TB-Ionene Polymer Membranes

membrane	$T_{\rm g}$ (°C)	d spacing (Å)	density
$[Im-TB(o)-Xy][Tf_2N]$	104	4.8	1.41
$[\operatorname{Im-TB}(o)\text{-}\operatorname{C}_{10}][\operatorname{Tf}_2\operatorname{N}]$	55	5.9	1.29
$[Im-TB(p)-Xy][Tf_2N]$	98	4.7	1.39
$[\operatorname{Im-TB}(p)\text{-}\operatorname{C}_{10}][\operatorname{Tf}_2\operatorname{N}]$	80	4.6	1.35

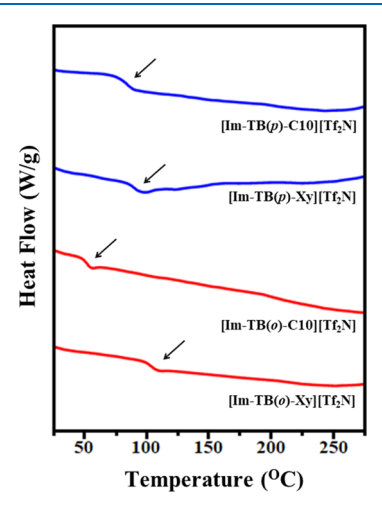


Figure 6. DSC curves of the Im-TB-Ionene polymers.

TB(o&p)- $C_{10}$ ][ $Tf_2N$ ] ionenes, similar values were also reported for imidazolium ionenes with butyl chains.<sup>37</sup> The lower  $T_g$  values were attributed to a looser packing of the ionene groups within the flexible aliphatic networks, suggesting that chain mobility of the ionenes was high, and hence, enhanced gas permeability was expected for the membrane with this combinational series. Most notably, a much lower  $T_g$  of 55 °C was observed for the ortho-positioned aliphatic Im-TB-Ionene polymer, [Im-TB(o)- $C_{10}$ ][ $Tf_2N$ ].

To further investigate the chemical structures and chain packing architectures of the newly developed ionenes, wide-angle X-ray diffraction (WAXD) was performed. As shown in Figure 7, there were no sharp peaks exhibited in all X-ray diffraction patterns, indicating the amorphous structures of Im-

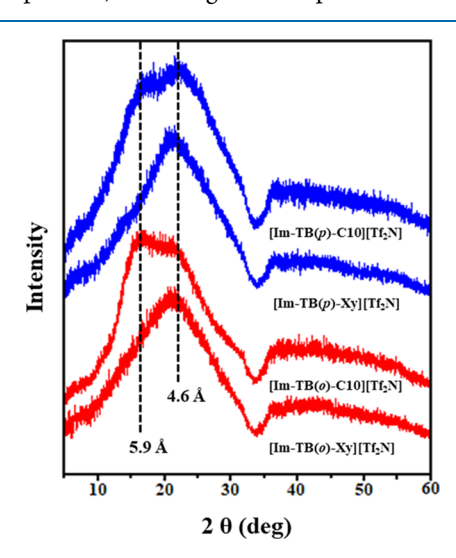


Figure 7. Wide-angle X-ray diffraction plots obtained from the Im-TB-Ionene membranes.

TB-Ionenes. Whereas both the aromatic copolymers [Im-TB(o&p)-Xy][Tf<sub>2</sub>N] displayed a single-peak distribution, a bimodal distribution was obtained for aliphatic copolymers [Im-TB(o&p)-C<sub>10</sub>][Tf<sub>2</sub>N], which is plausible because of the enhanced chain mobility of ionenes caused by alkyl chains. However, the intersegmental d spacing values of Im-TB-Ionenes calculated from the main halo ( $2\theta = 21-22^{\circ}$ ) remained constant irrespective of their molecular structure, except for [Im-TB(o)-C<sub>10</sub>][Tf<sub>2</sub>N] (Table 1). The main halo in [Im-TB(o)-C<sub>10</sub>][Tf<sub>2</sub>N] was shifted from  $2\theta$  of 21.5 to 17.2° and resulted in a high d spacing of 5.9 Å. The relatively higher d spacing of [Im-TB(o)-C<sub>10</sub>][Tf<sub>2</sub>N] can be attributed to the introduction of the alkyl groups into the ortho positions of the imidazolium—TB unit, which disrupts the chain packing of ionenes and increases the d spacing.

Generally, the d spacing represents the distance between the polymer chain segments, and the increase in the d spacing values of  $[\operatorname{Im-TB}(o)-C_{10}][\operatorname{Tf_2N}]$  might lead to a decrease in the density. The  $[\operatorname{Im-TB}(o)-C_{10}][\operatorname{Tf_2N}]$  yielded the lowest density among the four  $[\operatorname{Im-TB-Ionene}]$  polymers (Table 1). These results clearly suggested an increased free volume distribution and hence enhanced gas transport properties in the  $[\operatorname{Im-TB}(o)-C_{10}][\operatorname{Tf_2N}]$  membrane (see below).

**2.5.** Gas Transport Properties of Im-TB-Ionene Polymers. The pure gas permeabilities and permselectivities of the Im-TB-Ionene membranes were measured at 3 atm and 20 °C using a lab-made high-vacuum time-lag unit according to the constant volume—variable pressure method, as summarized in Table 2. The permeability of Im-TB-Ionenes

Table 2. Pure Gas Permeabilities  $(P)^a$  and Permselectivities  $(\alpha)$  of Im-TB-Ionene Polymer Membranes

membrane	$P_{\mathrm{CO}_2}$	$P_{ m N_2}$	$P_{\mathrm{CH_{4}}}$	$\alpha_{\mathrm{CO_2/N_2}}$	$lpha_{ m CO_2/CH_4}$		
$[Im-TB(o)-Xy][Tf_2N]$	1.99	0.077	0.026	25.8	76.5		
$[\operatorname{Im-TB}(o)\text{-}\operatorname{C}_{10}][\operatorname{Tf}_2\mathrm{N}]$	4.37	0.129	0.053	33.9	82.5		
$[Im-TB(p)-Xy][Tf_2N]$	2.02	0.084	0.038	24.1	53.2		
$[\operatorname{Im-TB}(p)-\operatorname{C}_{10}][\operatorname{Tf}_2\operatorname{N}]$	2.69	0.091	0.047	29.6	57.2		
$^aP$ in barrer, where 1 barrer = $10^{-10} (cm^3_{STP} cm)/(cm^2 s cmHg))$ . $^bAt$							
3 atm and 20 °C.							

follows the sequence of the kinetic diameter of the respective gas molecules:  $CO_2$  (3.3 Å) >  $N_2$  (3.6 Å) >  $CH_4$  (3.8 Å), a trend that indicates the size-selective chain packing of the newly developed ionenes due to the presence of TB units. As shown in Table 2, the gas permeabilities of aromatic segments containing ionenes displayed a similar result irrespective of their ortho and para substructures; for example, the CO<sub>2</sub> permeabilities of [Im-TB(o)-Xy][Tf<sub>2</sub>N] and [Im-TB(p)-Xy]-[Tf<sub>2</sub>N] were 1.99 and 2.02 barrer, respectively. In contrast, the aliphatic segments containing ionenes exhibited a dramatic increase in permeabilities, especially the ortho-positioned [Im- $TB(o)-C_{10}$  [Tf<sub>2</sub>N] ionene, due to the enhanced diffusivity as well as solubility coefficients (Table 3). [Im-TB(o)-C<sub>10</sub>][Tf<sub>2</sub>N] showed the best permeabilities among the four Im-TB-Ionenes; for example, the CO<sub>2</sub> permeability of [Im-TB(o)-C<sub>10</sub>][Tf<sub>2</sub>N] was 4.37 barrer (increased by about 2-fold). This provides further evidence that the alkyl groups in the ortho position of the imidazolium-TB unit effectively improve the flexibility in the polymer chain, which is consistent with the d spacing data and the thermal transition properties (lower  $T_g$ was obtained for  $[Im-TB(o)-C_{10}][Tf_2N]$ ).

Table 3. Pure Gas Diffusivity Coefficients<sup>a</sup> and Solubility Coefficients<sup>b</sup> with Their Ideal Selectivities<sup>c</sup>

membrane	$D_{\mathrm{CO}_2}$	$D_{ m N_2}$	$D_{\mathrm{CH_{4}}}$	$S_{CO_2}$	$S_{N_2}$	$S_{\mathrm{CH_{4}}}$	$D_{\mathrm{CO_2/N_2}}$	$D_{\mathrm{CO_2/CH_4}}$	$S_{\rm CO_2/N_2}$	$S_{\mathrm{CO_2/CH_4}}$
$[Im-TB(o)-Xy][Tf_2N]$	0.78	0.478	0.28	2.55	0.161	0.093	1.63	2.79	15.84	27.42
$[\operatorname{Im-TB}(o)\text{-}\operatorname{C}_{10}][\operatorname{Tf}_2\mathrm{N}]$	0.954	0.578	0.397	4.58	0.223	0.134	1.65	2.40	20.54	34.18
$[\operatorname{Im-TB}(p)\operatorname{-Xy}][\operatorname{Tf}_2\mathrm{N}]$	0.792	0.506	0.294	2.55	0.166	0.129	1.57	2.69	15.36	19.77
$[\operatorname{Im-TB}(p)\text{-}\operatorname{C}_{10}][\operatorname{Tf}_2\operatorname{N}]$	0.801	0.538	0.359	3.36	0.169	0.131	1.49	2.23	19.88	25.65
<sup>a</sup> Diffusivity coefficient (10 <sup>-8</sup> cm <sup>2</sup> /s). <sup>b</sup> Solubility coefficient (10 <sup>-2</sup> cm <sub>STP</sub> <sup>3</sup> cm <sup>-3</sup> cmHg <sup>-1</sup> ). <sup>c</sup> At 3 atm and 20 °C.										

(a) (b) 1000 1000 008 Upper Bound 2008 Upper Boun 1991 Upper Bound CO2/CH4 selectivity CO<sub>2</sub>/N<sub>2</sub> selectivity 100 100 10 Ionic Liquid-based Polymers Ionic Liquid-based Polymers Tröger's base-based polymers Tröger's base-based polymer 0.1 10 100 1000 10 100 1000 CO<sub>2</sub> permeability (Barrer) CO2 permeability (Barrer)

Figure 8. Robeson upper bound plot for comparing the (a) CO<sub>2</sub>/CH<sub>4</sub> and (b) CO<sub>2</sub>/N<sub>2</sub> separation performances of the Im-TB-Ionenes with other previously reported ionenes, poly(IL)s, and Tröger's base-containing polymers. Data were taken from refs 7 9 16 18 19 20 24 38 39, and 40.

On the other hand, the  $CO_2$  solubility in the Im-TB-Ionenes was much higher than the  $N_2$  or  $CH_4$  solubilities (Table 3). As a result, all the Im-TB-Ionenes obtained excellent  $CO_2/N_2$  and  $CO_2/CH_4$  permselectivities. [Im-TB(o)- $C_{10}$ ][Tf<sub>2</sub>N] showed an extraordinary high  $CO_2/CH_4$  permselectivity of 82.5.

The permeability—selectivity tradeoff results obtained for the CO<sub>2</sub>/CH<sub>4</sub> (Figure 8a) and CO<sub>2</sub>/N<sub>2</sub> (Figure 8b) separations in the membranes prepared from Im-TB-Ionenes were then compared to the upper bound of the Robeson plot.<sup>7,9</sup> Data from other imidazolium-based ionenes,<sup>38</sup> poly-(IL)s,<sup>24,39,40</sup> and Tröger's base-containing polymers <sup>16,18–20</sup> are also included for comparison. Although the permeability—selectivity values of the Im-TB-Ionenes fell below the upper bound lines for CO<sub>2</sub>/CH<sub>4</sub> and CO<sub>2</sub>/N<sub>2</sub>, their performances were comparable to the published data for poly(IL)s and ionenes. Although the separation performance of all the Im-TB-Ionenes for CO<sub>2</sub>/N<sub>2</sub> fell within the general range of other poly(IL)s and the ionenes, CO<sub>2</sub>/CH<sub>4</sub> outperformed the previously described ionene-based membranes (Figure 8a).

At the same time, a direct comparison of the newly developed Im-TB-Ionenes with the recently reported Tröger's base-containing polymers could not have been made because of the low permeability as well as the differences in the polymeric backbone. The relatively low gas permeabilities of these Im-TB-Ionenes might be due to either too much or insufficient amounts of the imidazolium—TB moiety present in the polymer backbone. These factors can be further optimized; the polymer backbone in Im-TB-Ionenes can potentially be fine-tuned by introducing more permeable polymers, such as polyimides. We foresee an extension study that uses bisindane-based dianhydrides (i.e., PIMs) and the benefits of regiochemistry of Im-TBs (i.e., use of ortho Im-TB) in our forthcoming works. Overall, the Im-TB-Ionenes prepared here

provide a novel approach to introducing imidazolium-TB groups into a variety of polymer structures for use in gas separations,  $^{18,41}$  CO $_2$  capture,  $^{42,43}$  catalysis,  $^{44}$  and electrochemical applications.  $^{45,46}$ 

## 3. CONCLUSIONS

We prepared a series of novel imidazolium-mediated Tröger's base-containing ionenes and successfully demonstrated the potential utility of the corresponding membranes for CO2 gas separation. This is the first example of the incorporation of Tröger's base groups into the imidazolium-ionene polymers to serve as a CO<sub>2</sub> selective separation membrane. We investigated the effects of Im-TB-Ionenes on the structures and properties of the polymers as well as the gas separation properties of the corresponding polymer membranes by varying the regiochemistry of imidazolium groups in TB units and the presence of aromatic and aliphatic co-monomers. All newly developed Im-TB-Ionene polymers exhibited high molecular weight, excellent solubility in polar organic solvents, and high thermal stability. The Im-TB-Ionene membranes showed superior CO<sub>2</sub>/CH<sub>4</sub> and CO<sub>2</sub>/N<sub>2</sub> selectivities with reasonable gas permeability yields. This simple strategy may be readily applied toward preparing more extraordinary polymer membranes for CO<sub>2</sub> separation applications.

## 4. EXPERIMENTAL SECTION

**4.1. Materials.** 2-Fluoronitrobenzene, 4-fluoronitrobenzene, and trifluoroacetic acid were purchased from Oakwood Chemical. Imidazole (99%) and 1,10-dibromodecane (>97%) were purchased from Aldrich. Potassium carbonate (99%, anhydrous) and Pd/C (10% on C, type 487) were purchased from BeanTown Chemical. Paraformaldehyde (>97%) was obtained from Alfa Aesar.  $\alpha$ ,  $\alpha'$ -Dichloro-p-xylene (>98%) was

purchased from TCI. Lithium bis-trifluoromethanesulfonimide (HQ-115) was purchased from 3M. Ethanol (200 proof), *N*-methylpyrrolidone (NMP) (ACS grade), and dimethylacetamide (DMAc) (ACS grade) were purchased from VWR. Celite 545 was purchased from Acros Organics. All other chemicals, unless otherwise noted, were obtained from commercial sources and used as received.

**4.2. Characterization.** <sup>1</sup>H NMR spectra were obtained on a Bruker Avance (500 MHz) instrument using DMSO- $d_6$  as a reference or internal deuterium lock. FT-IR spectra of the materials were recorded using a Perkin Elmer Spectrum 2 ATR-FTIR spectrometer in the range of 4000–400 cm $^{-1}$ . Molar masses were determined by matrix-assisted laser desorption ionization time-of-flight mass spectrometry (MALDI-TOF MS, Bruker Ultraflex instrument). Thermogravimetric analysis (TGA) of the ionene materials was conducted using Seiko TG-DTA 7300 by heating samples from room temperature to 700 °C at a heating rate of 10 °C/min under N<sub>2</sub> flow.

4.3. Synthesis of Imidazolium-Mediated TB-Based lonene Polymers (Im-TB-lonenes). 4.3.1. Synthesis of Imidazole-Aniline Derivatives (Ila and Ilb). For preparing the ortho derivative (IIa), imidazole (24.125 g, 354 mmol), 2fluoronitrobenzene (2-FNB, 25.000 g, 177 mmol), and potassium carbonate (K2CO3, 26.936 g, 195 mmol) were added with 300 mL of DMSO to a 1000 mL round-bottom flask equipped with a magnetic stir bar. The vessel was capped with a rubber stopper and vented with a needle through the cap to prevent the buildup of pressure in the flask upon heating. The reaction was heated to 110 °C while stirring for 24 h. The reaction was cooled to room temperature and poured into 700 mL of DI water to precipitate the product and remove excess imidazole. The product was filtered and then added back to a 500 mL round-bottom flask with 250 mL of Et<sub>2</sub>O. The product was left to stir in Et<sub>2</sub>O for 24 h to remove unreacted 2-FNB. The product was filtered and washed with 100 mL of Et<sub>2</sub>O and dried in a vacuum oven at 60 °C, yielding 1-(2-nitrophenyl)imidazoleproduct as a light yellow powder (26.973 g, 80%).

1-(2-nitrophenyl)imidazole (32.496 g, 172 mmol) was added with 300 mL of EtOH to a 500 mL round-bottom heavy-walled pressure vessel (Ace Glass) sealed with a threaded PTFE cap with a DuPont Kalrez O ring. Pd/C (1.100 g) was added to the flask, and the vessel was sealed with a Teflon screw cap fitted with Swagelok stainless steel fittings and tubing to accommodate for a gas inlet and a vacuum line. The reaction was set to stir with a H<sub>2</sub> feed (30 psi) for 48 h. The contents of the reaction were filtered through Celite to isolate the Pd/C for disposal, and the EtOH filtrate was transferred to a round-bottom flask. The solvent was removed via rotary evaporation, and the reduced product was dried under vacuum at 60 °C overnight to yield an off-white solid (17.621 g, 77%). <sup>1</sup>H NMR (360 MHz, DMSO- $d_6$ )  $\delta$  7.74 (t, J = 1.1 Hz, 1H), 7.30 (t, J = 1.3 Hz, 1H), 7.14 (ddd, J = 8.1, 7.3,1.6 Hz, 1H), 7.10 (t, J = 1.1 Hz, 1H), 7.03 (dd, J = 7.8, 1.6 Hz, 1H), 6.86 (dd, J = 8.1, 1.4 Hz, 1H), 6.64 (td, J = 7.5, 1.4 Hz, 1H), 5.06 (s, 2H).

The para derivative (IIb) was synthesized by the same method from imidazole (24.125 g, 354 mmol), 4-fluoronitrobenzene (4-FNB, 25.000 g, 177 mmol), and  $K_2CO_3$  (26.936 g, 195 mmol) in 300 mL of DMSO. The purified and dried product was collected as a light yellow powder (32.496 g, 97%). 1-(4-nitrophenyl)imidazole was reduced following the

same procedure in EtOH (300 mL) with Pd/C (0.95 g). The product was recovered via removal of EtOH and dried under vacuum to yield an off-white solid (22.164 g, 80%). <sup>1</sup>H NMR (500 MHz, DMSO- $d_6$ )  $\delta$  7.95 (s, 1H), 7.48 (s, 1H), 7.22 (d, 2H), 7.01 (s, 1H), 6.64 (d, I = 8.8, 2H), 5.26 (s, 2H).

4.3.2. Synthesis of Tröger's Base-Containing Imidazole Monomers (Im-TB, IIIa, and IIIb). Following a literature method for the preparation of ortho and para Im-TBs, <sup>32</sup> cooled (-15 °C) trifluoroacetic acid (200 mL) was added to IIa or IIb (10 g, 62.82 mmol) at -15 °C; subsequently, paraformaldehyde (4.72 g, 157.1 mmol) was added to the reaction mixture and allowed to stir at room temperature for 40 h. After the reaction, the resultant mixture was quenched by pouring into it crushed ice (900 g) followed by the addition of 30% aqueous ammonia solution (150 mL). The organic components were extracted with dichloromethane  $(3 \times 200)$ mL), washed with brine solution, and dried over anhydrous MgSO<sub>4</sub>, and the solvent was evaporated under reduced pressure to obtain a crude gummy compound. The product was purified by recrystallization from a MeOH-DCM mixture to give off-white crystals.

**Ha** (off-white crystals): Yield (75%). <sup>1</sup>H NMR (DMSO- $d_6$ ) δ 8.05 (s, 2H, J = 3.7, 2×N=CH−N), 7.60 (s, 2H, J = 7.4, 2 × N−CH=C), 7.20−6.94 (br signal, 2H, 2×C=CH−N, 6H, 6 × ArH), 4.37−4.29 (br signal, 4H, 2×N−CH<sub>2</sub>−C, 2 × N−CH−N), and 3.24 (s, 2H, 2 × N−CH<sub>2</sub>−C).

**IIb** (pale yellow crystals): Yield (72%).  $^{1}$ H NMR (DMSO- $d_6$ ) δ 8.05 (s, 2H, J = 3.7, 2 × N=CH−N), 7.60 (s, 2H, J = 7.6, 2 × N−CH=C), 7.21−6.95 (br signal, 2H, 2 × C=CH−N, 6H, 6 × ArH), 4.38−4.30 (br signal, 4H, 2 × N−CH<sub>2</sub>−C, 2 × N−CH−N), and 3.24 (s, 2H, 2 × N−CH<sub>2</sub>−C).

4.3.3. Synthesis of Four Im-TB-Ionenes. To a DMF (50 mL) solution of Im-TB IIIa or IIIb (4 g, 11.29 mmol), the corresponding equimolar comonomer (11.29 mmol, 1.98 g for  $\alpha,\alpha'$ -dichloro-p-xylene (DCXy) and 3.39 g for 1,10-dibromodecane (DBC<sub>10</sub>)was added into a heavy-walled round-bottom flask (Ace Glass) equipped with a magnetic stir bar. Then, the flask was sealed with a threaded PTFE cap and a DuPont Kalrez O ring. The reaction mixture was heated to 110 °C and allowed to stir for 24 h. After this time, the precipitated polymer product was cooled to room temperature, the remaining DMF was decanted, and deionized H<sub>2</sub>O was added directly to the flask. The vessel was heated to 40 °C while stirring to dissolve the dark brown solids. LiTf<sub>2</sub>N (8.1g, 28.2 mmol) was dissolved in 200 mL of DI water in a 500 mL Erlenmeyer flask, and the dissolved polymer product from the flask was poured into the aqueous LiTf<sub>2</sub>N solution, whereupon a precipitate immediately formed. The mixture was vigorously stirred with an overhead mechanical stirrer for 1 h, and the polymer was collected by filtration and dried in a vacuum oven for 36 h at 80 °C to give the desired Im-TB-Ionene polymer.

[Im-TB(o)-Xy][Tf<sub>2</sub>N]: Yield (86%). <sup>1</sup>H NMR (500 MHz, DMSO- $d_6$ )  $\delta$  9.91 (s, 2H, 2 × N=CH—N), 8.25 (s, 2H, 2 × N—CH=C), 8.04 (s, 2H, 2 × N—CH=C), 7.65–7.17 (br signal, 10H, ArH), 5.71–5.49 (br signal, 4H, ArCH<sub>2</sub>), 4.50–4.32 (br signal, 4H, 2 × N-CH<sub>2</sub>-C and 2 × N-CH-N), and 3.67–3.50 (br signal, 2H, 2 × N-CH<sub>2</sub>-C); (FT-IR)/cm<sup>-1</sup> 3082, 1690, 1480, 1320, 1190, 1050, 750, and 640.

[Im-TB(o)-C<sub>10</sub>][Tf<sub>2</sub>N]: Yield (83%). <sup>1</sup>H NMR (500 MHz, DMSO- $d_6$ )  $\delta$  9.67 (s, 2H, 2 × N=CH=N), 8.21 (s, 2H, 2 × N—CH=C), 8.10 (s, 2H, 2 × N—CH=C), 7.48-7.15 (br signal, 10H, ArH), 4.40-4.30 (br signal, 6H, 4 × N-CH<sub>2</sub>-C, 2 × N-CH-N), 3.59 (br signal, 2H, 2 × N-CH<sub>2</sub>-C), 1.94 (s,

2H,  $2 \times C - CH_2 - C$ ), and 1.37 (s, 16H, 16  $\times$  C - CH<sub>2</sub> - C); (FT-IR)/cm<sup>-1</sup> 3082, 2860, 1690, 1480, 1320, 1190, 1050, 750, and 640.

[Im-TB(p)-Xy][Tf<sub>2</sub>N]: Yield (85%). <sup>1</sup>H NMR (500 MHz, DMSO- $d_6$ )  $\delta$  10.17–9.95 (br signal, 2H, 2 × N=CH-N) 8.63–8.28 (br signal, 4H, 4 × N-CH=C) 8.10–7.62 (br signal, 10H, ArH) 5.53–5.16 (br signal, 8H, 2 × N-CH<sub>2</sub>-C, 2 × N-CH-N and 4 × ArCH<sub>2</sub>), and 3.61–3.5 (br signal, 2H, 2 × N-CH<sub>2</sub>-C); (FT-IR)/cm<sup>-1</sup> 3082, 1690, 1480, 1320, 1190, 1050, 750, and 640.

[Im-TB(p)-C<sub>10</sub>][Tf<sub>2</sub>N]: Yield (82%). <sup>1</sup>H NMR (500 MHz, DMSO- $d_6$ )  $\delta$  10.10–9.95 (br signal, 2H, 2 × N=CH-N) 8.62–8.27 (br signal, 4H, 4 × N—CH=C) 8.09–7.60 (br signal, 10H, ArH) 4.30–4.17 (br signal, 6H, 4 × N–CH<sub>2</sub>–C, 2 × N–CH–N), 3.58 (br signal, 2H, 2 × N–CH<sub>2</sub>–C), 1.93 (s, 2H, 2 × C–CH<sub>2</sub>–C), and 1.35 (s, 16H, 16 × C–CH<sub>2</sub>–C); (FT-IR)/cm<sup>-1</sup> 3082, 2860, 1690, 1480, 1320, 1190, 1050, 750, and 640.

**4.4. Synthesis Im-TB-Ionene Membranes.** All the Im-TB-Ionene membranes were prepared by the solution-casting method using DMAc as solvent. The corresponding ionene polymers (1.2 g, 10 wt %) were dissolved in DMAc (10.8 g, 90 wt %) and sonicated at 30 °C until they formed completely homogeneous solutions. The resultant solutions were filtered through a cotton plug to ensure that the solution was free of any dust particles and poured onto a Teflon block. The Teflon plates were then placed in an oven, covered with aluminum foil having small holes, underwent slow solvent evaporation at 40 °C for 96 h, and further dried at 60 °C for 48 h in a vacuum oven. After becoming completely dried, the membranes were peeled off from the Teflon plate and then dried at ambient temperature. The membrane thickness was controlled to be 90 to 110  $\mu$ m.

**4.5. Membrane Characterization.** The densities of the membranes (g cm<sup>-3</sup>) were determined experimentally using a top-loading electronic Mettler Toledo balance (XP205, Mettler Toledo, Switzerland) coupled with a density kit based on Archimedes' principle. The samples were weighed in air, and a known-density liquid (high-purity heptane) was used. All measurements were carried out at room temperature by the buoyancy method, and the density was calculated as follows

$$\rho_{\rm polymer} = \frac{W_0}{W_0 - W_1}$$

where  $W_0$  and  $W_1$  are the membrane weights in air and water, respectively. The liquid sorption of the Im-TB-Ionene membranes was not considered due to their extremely low swelling property.

The glass transition temperature ( $T_{\rm g}$ ) of each Im-TB-Ionene polymer was measured by DSC (TA Instruments, DSC Q20) from 20 to 300 °C with a scan rate of 10 °C min<sup>-1</sup> under N<sub>2</sub>.

The wide-angle X-ray diffraction (WAXD) patterns of the membranes were measured using a Bruker D8 Discover diffractometer by employing a scanning rate of  $4^{\circ}$ /min in a  $2\theta$  range from 5 to  $60^{\circ}$  with a Co K $\alpha$ 1 X-ray ( $\lambda$  = 0.17886) source. The d spacing values were calculated using Bragg's law ( $d = \lambda/2\sin\theta$ ).

**4.6. Gas Separation Measurements.** The pure gas permeation measurements were performed to determine the gas separation abilities of the newly developed Im-TB-Ionene polymer membranes using high-vacuum time-lag apparatus based on the constant volume—variable pressure method. The

construction and operation of this measurement unit were already discussed in our previous works. 39,47 The only addition to the construction was that Im-TB-Ionene membranes were "masked" on both sides using adhesive aluminum tape to confine gas permeation through a fixed membrane area of <sup>1</sup>/<sub>2</sub> in. diameter, as described elsewhere. 48 All measurements were ideal (i.e., single gas) and performed at 20 °C, and the feed pressure was ~3 atm (~45 psia) against an initial downstream vacuum (<0.01 psia). Pressures and temperatures were measured and recorded using the most recent version of LabVIEW software (National Instruments). After each measurement, the unit was held under dynamic vacuum (<0.01 psia) for at least 16 h at ambient temperature. The pressure rise versus time transient signals of the permeate side, equipped with a pressure transducer, were recorded and passed to a desktop computer through a shield data cable. The permeability coefficient was determined from the linear slope of the downstream pressure rise versus time plot (dp/dt)according to the following equation

$$P = \frac{273}{76} \times \frac{Vl}{ATp_0} \times \frac{dp}{dt}$$

where P is the permeability expressed in barrer (1 barrer =  $10^{-10}$  cm<sub>STP</sub><sup>3</sup> cm cm<sup>-2</sup> s<sup>-1</sup> cmHg<sup>-1</sup>), V (cm<sup>3</sup>) is the downstream volume, l (cm) is the membrane thickness, A (cm<sup>2</sup>) is the effective area of the membrane, T (K) is the temperature of measurement,  $p_0$  (Torr) is the pressure of the feed gas in the upstream chamber, and dp/dt is the rate of the pressure rise in the steady state. Assuming the solution—diffusion (S–D) mechanism, the diffusivity ( $D_i$ ) of each gas was calculated from the time lag ( $\Theta$ ) and membrane thickness (l), and the solubility ( $S_i$ ) of each gas was calculated as the quotient of  $P_i$  and  $D_i$ . The pure gas permeability, solubility, and diffusivity selectivity ( $\alpha_{i,j}$ ) for a given gas pair (e.g.,  $CO_2/N_2$ ) were calculated as  $P_i/P_i$ ,  $S_i/S_i$ , and  $D_i/D_i$ , respectively.

#### ASSOCIATED CONTENT

## **S** Supporting Information

The Supporting Information is available free of charge on the ACS Publications website at DOI: 10.1021/acsomega.8b03700.

Molar masses of ionene polymers with MALDI-TOF-MS spectra, NMR spectra of monomers, and solubility properties (PDF)

## AUTHOR INFORMATION

#### **Corresponding Author**

\*E-mail: jbara@eng.ua.edu.

ORCID ®

Irshad Kammakakam: 0000-0002-8464-828X

Jason E. Bara: 0000-0002-8351-2145

**Notes** 

The authors declare no competing financial interest.

#### ACKNOWLEDGMENTS

This material is based upon the work supported by the U.S. Department of Energy, Office of Science, Office of Basic Energy Sciences, Separation Science program under award no. DE-SC0018181. Additional support from the NASA Marshall Space Flight Center (CAN 80MSFC18M0041) and NSF CHE-1726812 from the Major Research Instrumentation

Program for purchase of the MALDI/TOF-TOF mass spectrometer is gratefully acknowledged.

#### REFERENCES

- (1) Koros, W. J.; Fleming, G. K. Membrane-Based Gas Separation. *J. Membr. Sci.* **1993**, 83, l–80.
- (2) Bernardo, P.; Drioli, E.; Golemme, G. Membrane Gas Separation: A Review/State of the Art. *Ind. Eng. Chem. Res.* **2009**, 48, 4638–4663.
- (3) Sanders, D. F.; Smith, Z. P.; Guo, R.; Robeson, L. M.; McGrath, J. E.; Paul, D. R.; Freeman, B. D. Energy-Efficient Polymeric Gas Separation Membranes for a Sustainable Future: A Review. *Polymer* **2013**, *54*, 4729–4761.
- (4) Cecopieri-Gómez, M. L.; Palacios-Alquisira, J.; Domínguez, J. M. On the Limits of Gas Separation in CO<sub>2</sub>/CH<sub>4</sub>, N<sub>2</sub>/CH<sub>4</sub> and CO<sub>2</sub>/N<sub>2</sub> Binary Mixtures Using Polyimide Membranes. *J. Membr. Sci.* **2007**, 293, 53–65.
- (5) Du, N.; Park, H. B.; Dal-Cin, M. M.; Guiver, M. D. Advances in High Permeability Polymeric Membrane Materials for CO<sub>2</sub> Separations. *Energy Environ. Sci.* **2012**, *5*, 7306–7322.
- (6) Faiz, R.; Li, K. Polymeric Membranes for Light Olefin/Paraffin Separation. *Desalination* **2012**, 287, 82–97.
- (7) Robeson, L. M. Correlation of Separation Factor Versus Permeability for Polymeric Membranes. *J. Membr. Sci.* **1991**, *62*, 165–185.
- (8) Freeman, B. D. Basis of Permeability/Selectivity Tradeoff Relations in Polymeric Gas Separation Membranes. *Macromolecules* **1999**, 32, 375–380.
- (9) Robeson, L. M. The Upper Bound Revisited. *J. Membr. Sci.* **2008**, 320, 390–400.
- (10) Budd, P. M.; Msayib, K. J.; Tattershall, C. E.; Ghanem, B. S.; Reynolds, K. J.; McKeown, N. B.; Fritsch, D. Gas Separation Membranes from Polymers of Intrinsic Microporosity. *J. Membr. Sci.* **2005**, 251, 263–269.
- (11) Du, N.; Robertson, G. P.; Song, J.; Pinnau, I.; Guiver, M. D. High-Performance Carboxylated Polymers of Intrinsic Microporosity (PIMs) with Tunable Gas Transport Properties. *Macromolecules* **2009**, 42, 6038–6043.
- (12) McKeown, N. B.; Budd, P. M. Exploitation of Intrinsic Microporosity in Polymer-Based Materials. *Macromolecules* **2010**, 43, 5163–5176.
- (13) Ghanem, B. S.; McKeown, N. B.; Budd, P. M.; Selbie, J. D.; Fritsch, D. High-Performance Membranes from Polyimides with Intrinsic Microporosity. *Adv. Mater.* **2008**, *20*, 2766–2771.
- (14) Bezzu, C. G.; Carta, M.; Tonkins, A.; Jansen, J. C.; Bernardo, P.; Bazzarelli, F.; McKeown, N. B. A Spirobifluorene-Based Polymer of Intrinsic Microporosity with Improved Performance for Gas Separation. *Adv. Mater.* **2012**, *24*, 5930–5933.
- (15) Carta, M.; Malpass-Evans, R.; Croad, M.; Rogan, Y.; Jansen, J. C.; Bernardo, P.; Bazzarelli, F.; McKeown, N. B. An Efficient Polymer Molecular Sieve for Membrane Gas Separations. *Science* **2013**, 339, 303–307.
- (16) Zhuang, Y.; Seong, J. G.; Do, Y. S.; Jo, H. J.; Cui, Z.; Lee, J.; Lee, Y. M.; Guiver, M. D. Intrinsically Microporous Soluble Polyimides Incorporating Tröger's Base for Membrane Gas Separation. *Macromolecules* **2014**, *47*, 3254–3262.
- (17) Williams, R.; Burt, L. A.; Esposito, E.; Jansen, J. C.; Tocci, E.; Rizzuto, C.; Lanč, M.; Carta, M.; McKeown, N. B. A Highly Rigid and Gas Selective Methanopentacene-based Polymer of Intrinsic Microporosity Derived from Tröger's base Polymerization. *J. Mater. Chem. A* 2018, 6, 5661–5667.
- (18) Wang, Z.; Wang, D.; Jin, J. Microporous Polyimides with Rationally Designed Chain Structure Achieving High Performance for Gas Separation. *Macromolecules* **2014**, *47*, 7477–7483.
- (19) Wang, Z.; Wang, D.; Zhang, F.; Jin, J. Tröger's Base-Based Microporous Polyimide Membranes for High-Performance Gas Separation. ACS Macro Lett. 2014, 3, 597–601.
- (20) Ma, X.; Abdulhamid, M.; Miao, X.; Pinnau, I. Facile Synthesis of a Hydroxyl-Functionalized Tröger's Base Diamine: A New Building

- Block for High-Performance Polyimide Gas Separation Membranes. *Macromolecules* **2017**, *50*, 9569–9576.
- (21) Bara, J. E.; Carlisle, T. K.; Gabriel, C. J.; Camper, D.; Finotello, A.; Gin, D. L.; Noble, R. D. Guide to CO<sub>2</sub>Separations in Imidazolium-Based Room-Temperature Ionic Liquids. *Ind. Eng. Chem. Res.* **2009**, 48, 2739–2751.
- (22) Scovazzo, P. Determination of The Upper Limits, Benchmarks, and Critical Properties for Gas Separations Using Stabilized Room Temperature Ionic Liquid Membranes (SILMs) for the Purpose of Guiding Future Research. *J. Membr. Sci.* **2009**, 343, 199–211.
- (23) Cserjési, P.; Nemestóthy, N.; Bélafi-Bakó, K. Gas Separation Properties of Supported Liquid Membranes Prepared with Unconventional Ionic Liquids. *J. Membr. Sci.* **2010**, 349, 6–11.
- (24) Bara, J. E.; Gabriel, C. J.; Hatakeyama, E. S.; Carlisle, T. K.; Lessmann, S.; Noble, R. D.; Gin, D. L. Improving CO<sub>2</sub> Selectivity in Polymerized Room-Temperature Ionic Liquid Gas Separation Membranes Through Incorporation of Polar Substituents. *J. Membr. Sci.* 2008, 321, 3–7.
- (25) Li, P.; Coleman, M. R. Synthesis of Room Temperature Ionic Liquids Based Random Copolyimides for Gas Separation Applications. *Eur. Polym. J.* **2013**, *49*, 482–491.
- (26) Kammakakam, I.; Kim, H. W.; Nam, S. Y.; Park, H. B.; Kim, T.-H. Alkyl Imidazolium-Functionalized Cardo-Based Poly(ether ketone)s as Novel Polymer Membranes for  $O_2/N_2$  and  $CO_2/N_2$  Separations. *Polymer* **2013**, *54*, 3534–3541.
- (27) Liang, L.; Gan, Q.; Nancarrow, P. Composite Ionic Liquid and Polymer Membranes for Gas Separation at Elevated Temperatures. *J. Membr. Sci.* **2014**, *450*, 407–417.
- (28) Gan, Q.; Rooney, D.; Xue, M.; Thompson, G.; Zou, Y. An Experimental Study of Gas Transport and Separation Properties of Ionic Liquids Supported on Nanofiltration Membranes. *J. Membr. Sci.* **2006**, 280, 948–956.
- (29) Supasitmongkol, S.; Styring, P. High CO<sub>2</sub> Solubility in Ionic Liquids and a Tetraalkylammonium-based Poly(ionic liquid). *Energy Environ. Sci.* **2010**, *3*, 1961–1972.
- (30) Hu, X.; Tang, J.; Blasig, A.; Shen, Y.; Radosz, M. CO<sub>2</sub> Permeability, Diffusivity and Solubility in Polyethylene Glycol-grafted Polyionic Membranes and Their CO<sub>2</sub> Selectivity Relative to Methane and Nitrogen. *J. Membr. Sci.* **2006**, *281*, 130–138.
- (31) Mittenthal, M. S.; Flowers, B. S.; Bara, J. E.; Whitley, J. W.; Spear, S. K.; Roveda, J. D.; Wallace, D. A.; Shannon, M. S.; Holler, R.; Martens, R.; Daly, D. T. Ionic Polyimides: Hybrid Polymer Architectures and Composites with Ionic Liquids for Advanced Gas Separation Membranes. *Ind. Eng. Chem. Res.* **2017**, *56*, 5055–5069.
- (32) Sathyanarayana, A.; Prabusankar, G. Facile Access to Imidazole and Imidazolium Substituted Dibenzo-Diazocines. *New J. Chem.* **2014**, *38*, 3613–3621.
- (33) Bara, J. E.; O'Harra, K. E.; Durbin, M. M.; Dennis, G. P; Jackson, E. M.; Thomas, B.; Odutola, J. A. Synthesis and Characterization of Ionene-Polyamide Materials as Candidates for New Gas Separation Membranes. *MRS Adv.* **2018**, *3*, 3091–3102.
- (34) Zhao, S.; Liao, J.; Li, D.; Wang, X.; Li, N. Blending of Compatible Polymer of Intrinsic Microporosity (PIM-1) with Tröger's Base Polymer for Gas Separation Membranes. *J. Membr. Sci.* **2018**, *566*, 77–86.
- (35) Kammakakam, I.; Rao, A. H. N.; Yoon, H. W.; Nam, S.; Park, H. B.; Kim, T.-H. An Imidazolium-Based Ionene Blended with Crosslinked PEO as a Novel Polymer Membrane for Selective CO<sub>2</sub> Separation. *Macromol. Res.* **2014**, *22*, 907–916.
- (36) Smith, T. W.; Zhao, M.; Yang, F.; Smith, D.; Cebe, P. Imidazole Polymers Derived from Ionic Liquid 4-Vinylimidazolium Monomers: Their Synthesis and Thermal and Dielectric Properties. *Macromolecules* **2013**, *46*, 1133–1143.
- (37) Erdmenger, T.; Perevyazko, I.; Vitz, J.; Pavlov, G.; Schubert, U. S. Microwave-Assisted Synthesis of Imidazolium Ionenes and Their Application as Humidity Absorbers. *J. Mater. Chem.* **2010**, *20*, 3583–3585.
- (38) Carlisle, T. K.; Bara, J. E.; Lafrate, A. L.; Gin, D. L.; Noble, R. D. Main-Chain Imidazolium Polymer Membranes for CO<sub>2</sub> Separa-

tions: An Initial Study of a New Ionic Liquid-Inspired Platform. J. Membr. Sci. 2010, 359, 37–43.

- (39) Bara, J. E.; Lessmann, S.; Gabriel, C. J.; Hatakeyama, E. S.; Noble, R. D.; Gin, D. L. Synthesis and Performance of Polymerizable Room-Temperature Ionic Liquids as Gas Separation Membranes. *Ind. Eng. Chem. Res.* **2007**, *46*, 5397–5404.
- (40) Tomé, L. C.; Aboudzadeh, M. A.; Rebelo, L. P. N.; Freire, C. S. R.; Mecerreyes, D.; Marrucho, I. M. Polymeric Ionic Liquids with Mixtures of Counter-Anions: A New Straightforward Strategy for Designing Pyrrolidinium-based CO<sub>2</sub> Separation Membranes. *J. Mater. Chem. A* 2013, 1, 10403–10411.
- (41) Carta, M.; Croad, M.; Jansen, J. C.; Bernardo, P.; Clarizia, G.; McKeown, N. B. Synthesis of Cardo-Polymers Using Tröger's Base Formation. *Polym. Chem.* **2014**, *5*, 5255–5261.
- (42) Zhu, X.; Do-Thanh, C.-L.; Murdock, C. R.; Nelson, K. M.; Tian, C.; Brown, S.; Mahurin, S. M.; Jenkins, D. M.; Hu, J.; Zhao, B.; Liu, H.; Dai, S. Efficient CO<sub>2</sub> Capture by a 3D Porous Polymer Derived from Tröger's Base. *ACS Macro Lett.* **2013**, *2*, 660–663.
- (43) Del Regno, A.; Gonciaruk, A.; Leay, L.; Carta, M.; Croad, M.; Malpass-Evans, R.; McKeown, N. B.; Siperstein, F. R. Polymers of Intrinsic Microporosity Containing Tröger Base for CO<sub>2</sub> Capture. *Ind. Eng. Chem. Res.* **2013**, *52*, 16939–16950.
- (44) Carta, M.; Croad, M.; Bugler, K.; Msayib, K. J.; McKeown, N. B. Heterogeneous Organocatalysts Composed of Microporous Polymer Networks Assembled by Tröger's Base Formation. *Polym. Chem.* **2014**, *5*, 5262–5266.
- (45) Xia, F.; Pan, M.; Mu, S.; Malpass-Evans, R.; Carta, M.; McKeown, N. B.; Attard, G. A.; Brew, A.; Morgan, D. J.; Marken, F. Polymers of Intrinsic Microporosity in Electrocatalysis: Novel Pore rigidity Effects and Lamella Palladium Growth. *Electrochim. Acta* **2014**, *128*, 3–9.
- (46) Rong, Y.; Malpass-Evans, R.; Carta, M.; McKeown, N. B.; Attard, G. A.; Marken, F. Intrinsically Porous Polymer Protects Catalytic Gold Particles for Enzymeless Glucose Oxidation. *Electroanalysis* **2014**, *26*, 904–909.
- (47) Bara, J. E.; Kaminski, A. K.; Noble, R. D.; Gin, D. L. Influence of Nanostructure on Light Gas Separations in Cross-Linked Lyotropic Liquid Crystal Membranes. *J. Membr. Sci.* **2007**, 288, 13–19.
- (48) Li, P.; Paul, D. R.; Chung, T. S. High Performance Membranes Based on Ionic Liquid Polymers for CO<sub>2</sub> Separation from the Flue Gas. *Green Chem.* **2012**, *14*, 1052–1063.